Beyond Random Walks: Revealing the Fractal Memory of Financial Markets

Remiat Alexandre

May 12, 2025

Abstract

This paper presents a study on long-term memory processes in financial time series using Hurst estimation methods, specifically the traditional R/S statistic (Rescaled Range analysis) and the modified R/S statistic (M-R/S). The R/S statistic and the modified R/S statistic are computed to determine the presence of long-term memory in the time series data. The inferential outcomes remain inconclusive, as the computation of a solitary static Hurst exponent across the entire time series lacks sufficient robustness and can be influenced by the length of the series, the presence of trends, or structural breaks. To address these issues, we employed the Multifractal Detrended Fluctuation Analysis (MF-DFA) to investigate the local behavior of the series and characterize its multifractal spectrum. The multifractal spectrum reveals that the series might exhibit multifractal properties. To take advantage of this, we propose a trading strategy based on the Hurst exponent, the multifractal spectrum and a proposed inefficiency index that combines the multifractality and the Hurst exponent. We examine trading pairs whose patterns or behaviors vary depending on the scale at which the data is viewed. The inefficiency index is used as a filter to determine the significance of our trading signal. The strategy (ModifOverlap120) outperforms the long-only S&P 500 portfolio, the long-only Russell 2000 portfolio and 50/50 portfolio. Moreover, the strategies that used the inefficiency index as a filter outperform the strategies that did not use it on max drawdown and volatility therefore confirming the hypothesis that our inefficiency index behaves as a risk management tool.

1 Introduction

The Hurst exponent is a crucial tool for analyzing long-term memory and self-similarity in stochastic processes. Originally introduced by Harold Hurst in the 1950s for studying river flows, this measure has since been widely adopted in various fields such as physics, environmental science and finance. In financial markets, the Hurst exponent serves as an indicator to determine whether a time series exhibits long-range dependence (a value greater than 0.5) or mean-reverting behavior (a value less than 0.5), a value equals to 0.5 indicates that the series follows a pure random walk, characteristic of standard Brownian motion.

The most common method for estimating the Hurst exponent is through Rescaled Range (R/S) analysis, introduced by Hurst and later refined by Mandelbrot. However, the traditional R/S statistic has its limitations, particularly its sensitivity to short-term memory effects, which can obscure the detection of long-term memory. To mitigate these issues, Lo (1991) proposed a modified version of the R/S statistic (M-R/S) that better accounts for short-term autocorrelation.

In this study, we apply both the R/S method and the M-R/S to estimate the Hurst exponent on financial time series and we complement our analysis with Multifractal Detrended Fluctuation Analysis (MF-DFA), which examines the local behavior of the series and characterizes its multifractal spectrum.

The Fractional Brownian motion (fBm) is often used as a benchmark model for processes with memory, as it embodies the scaling properties and persistence typically observed in long-memory data. While fBm provides a theoretical framework for understanding these phenomena, our study focuses on practical estimation methods.

2 Fractional Brownian Motion

Fractional Brownian motion (fBm) is a generalization of standard Brownian motion that introduces dependence in increments, making it suitable for modeling processes with memory effects. It is a continuous-time Gaussian process $X_H(t)$ where $H \in [0, 1]$ corresponds to the Hurst exponent with the following properties:

— The process exhibits self-similarity, meaning that for any scaling factor c, $c \in \mathbb{R}^+$, the rescaled process satisfies:

$$X_H(ct) \overset{d}{=} c^H X_H(t). \tag{1}$$

where the symbol $\overset{d}{=}$ denotes equality in distribution, meaning that the statistical properties of $X_H(ct)$ and $c^H X_H(t)$ are identical.

— The increments $X_H(t) - X_H(s)$ follow a normal distribution with mean zero and variance :

$$\mathbb{E}\left[(X_H(t) - X_H(s))^2\right] = \sigma^2 |t - s|^{2H}, \tag{2}$$

where H is the Hurst exponent.

— When $H = 0.5$, fBm reduces to classical Brownian motion.

— For $H > 0.5$, the process exhibits long-term positive autocorrelation, meaning that an increase in the past tends to be followed by further increases.

— For $H < 0.5$, the process has anti-persistent behavior, where an increase in the past is more likely to be followed by a decrease.

The covariance function of fBm is given by (see Section 6.4 for demonstration):

$$C_H(t,s) = \frac{\sigma^2}{2}\left(t^{2H} + s^{2H} - |t-s|^{2H}\right), \tag{3}$$

which accounts for the dependence structure of the process. The Hurst exponent H plays a critical role in determining the smoothness and correlation properties of fBm:

— **For small H values** ($H < 0.5$), the process is highly erratic, with rapid changes and weak memory effects.

— **For large H values** ($H > 0.5$), the trajectory becomes smoother, and the process exhibits long-range dependence.

2.1 Simulation of Fractional Brownian Motion

In this simulation, we aim to generate fractional Brownian motion (fBm) to better understand how the autocorrelation decays as a function of the Hurst exponent H. By simulating paths for different values of H, we can observe how the memory and persistence properties of the process vary. To generate the fractional Brownian motion (fBm), we use a Cholesky decomposition-based approach. The covariance matrix of fBm is given by (3):

where H is the Hurst exponent, which determines the degree of long-term dependence in the process.

The steps of the simulation are as follows:

1. Define a time grid of N points between 0 and T.
2. Compute the covariance matrix using (3).
3. Apply Cholesky decomposition to obtain a lower triangular matrix L.
4. Generate a vector W of standard normal random variables.
5. Obtain the fBm path by computing $X = LW$.

The params used for this simulation are N = 1000 number of points, T = 1 day, Hurst exponents $H = 0.2, 0.35, 0.5, 0.65, 0.8$, the number of lag for the autocorrelation is 40.

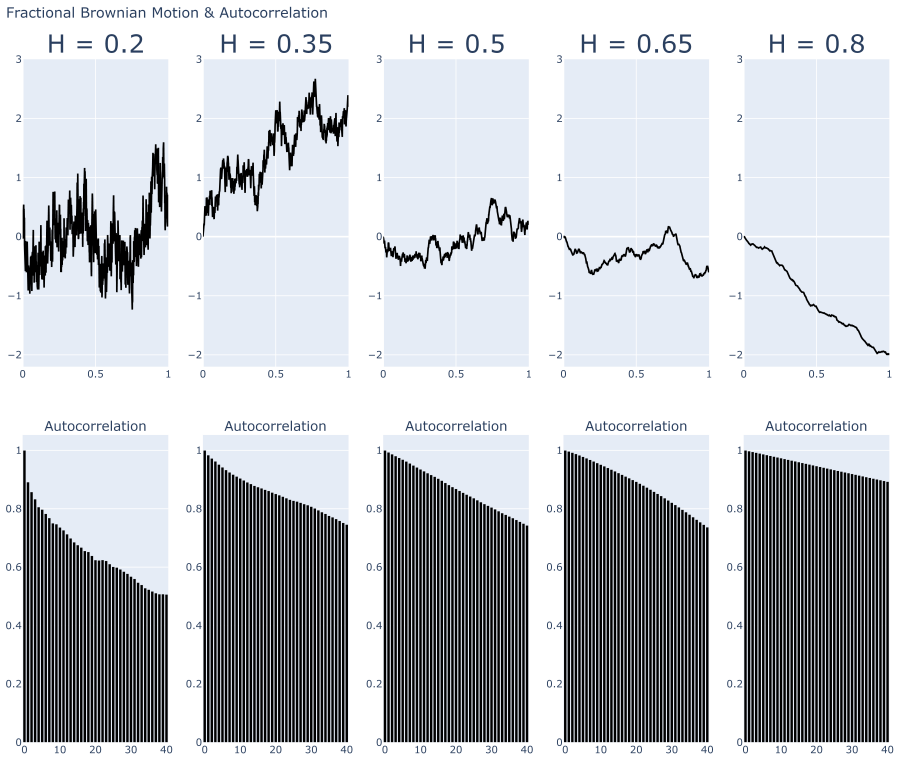

Figure 1 – Simulation of fractional Brownian motion with different Hurst exponent and its autocorrelation function. Value of H = 0.2, 0.35, 0.5, 0.65, 0.8 and 1000 points is simulated over a day.

The behavior of the fractional Brownian motion varies significantly with the Hurst exponent H.

When H is small (close to 0), the fBm exhibits high local variability, resulting in a highly granular trajectory with frequent fluctuations. The autocorrelation of increments decays rapidly, indicating that future values are weakly influenced by past values. This suggests a short-memory process, similar to standard Brownian motion.

As H increases, the autocorrelation decays more slowly, meaning that past values have a more significant impact on future values. This introduces a form of long-term dependence, where the process exhibits persistent trends. Consequently, the fBm trajectory appears smoother, with larger coherent movements and fewer abrupt changes.

In summary, a lower H leads to a more irregular and noisy path, characteristic of short-memory processes, while a higher H results in a smoother trajectory with stronger persistence.

2.2 R/S and Modified R/S Analysis

The R/S (Rescaled Range) analysis, introduced by Hurst and developed in various works by Mandelbrot, is certainly the most well-known method for estimating the Hurst exponent H. This statistic is defined as the range of the partial sums of deviations from the mean of a time series divided by its standard deviation. Consider a time series Y_t, $t = 1, \ldots, T$, with mean $\bar{Y}$. The range R is defined as:

$$R = \max_{1 \le j \le T} \left(Y_j - \bar{Y} \right) - \min_{1 \le j \le T} \left(Y_j - \bar{Y} \right). \tag{4}$$

The R/S statistic is then computed by dividing the range by the standard deviation s_T of the series:

$$Q_T = \frac{R}{s_T} = \frac{\max_{1\leq j\leq T}\left(Y_j - \bar{Y}\right) - \min_{1\leq j\leq T}\left(Y_j - \bar{Y}\right)}{s_T}, \quad \text{with } s_T = \sqrt{\frac{1}{T}\sum_{j=1}^{T}\left(Y_j - \bar{Y}\right)^2}. \tag{5}$$

Empirical studies by Mandelbrot and Wallis (1969b) have shown that Q_T scales with the number of observations T according to

$$Q_T \sim T^H, \tag{6}$$

which implies that by taking logarithms, the Hurst exponent H can be obtained from

$$H \sim \frac{\log(Q_T)}{\log(T)}. \tag{7}$$

Unfortunately, the asymptotic distribution of the R/S statistic is not known, making it difficult to establish a statistical test for the null hypothesis of short memory against the alternative hypothesis of long memory. Moreover, the R/S statistic does not explicitly account for short-term autocorrelation in the data, which can inflate (or reduce) the overall range and misrepresent the true variability of the series. Standard deviation estimates likewise ignore autocorrelated structure over short horizons, compounding the bias. As a result, the R/S measure can erroneously detect long memory when, in fact, short-term effects are responsible. This shortfall motivated Lo's Modified R/S procedure.

2.3 Modified R/S Analysis

The modified R/S statistic, denoted by $\tilde{Q}_T$, is defined as:

$$\tilde{Q}_T = \frac{R}{\hat{\sigma}_T(q)}, \tag{8}$$

where

$$\hat{\sigma}_T(q) = \sqrt{\frac{1}{T}\sum_{j=1}^{T}(Y_j - \bar{Y})^2 + \frac{2}{T}\sum_{j=1}^{T} w_j(q)\left[\sum_{i=j+1}^{T}(Y_i - \bar{Y})(Y_{i-j} - \bar{Y})\right]}, \tag{9}$$

and

$$w_j(q) = 1 - \frac{j}{q+1}. \tag{10}$$

This statistic differs from the traditional R/S statistic only by its denominator. In the presence of autocorrelation, the denominator does not solely represent the sum of the variances of the individual terms, but also includes autocovariances weighted according to lags q, with the weights $w_j(q)$ suggested by Newey and West (1987). Moreover, Andrews (1991) proposed a rule for choosing q:

$$q = [k_T] \quad \text{where} \quad k_T = \left(\frac{3T}{2}\right)^{\frac{1}{3}}\left(\frac{2\rho_1}{1-\rho_1^2}\right)^{\frac{2}{3}}, \tag{11}$$

where $[k_T]$ is the integer part of k_T, and ρ_1 is the first-order autocorrelation coefficient.

Unlike the classical R/S analysis, the limiting distribution of the modified R/S statistic is known. The statistic V, defined by

$$V = \frac{\tilde{Q}_T}{\sqrt{T}}, \tag{12}$$

converges to the range of a Brownian bridge over the unit interval. This convergence allows one to perform a statistical test for the null hypothesis of short memory against the alternative hypothesis of long memory by referring to the critical value table provided by Lo (1991), shown in Table 3. Therefore, accepting the null hypothesis implies that the series lacks the slow-decaying dependencies characteristic of long memory processes.

2.4 Data

The data used in this analysis is monthly and consists of the historical closing prices of five major stock market indices: the S&P 500, Russell 2000, FTSE 100, Nikkei 225, and the DAX. The data spans the period from September 10th, 1987, to February 28th, 2025.

For each index, the closing price time series was transformed using the natural logarithm to obtain a series of log prices. Additionally, a stationarity test was conducted on the log prices series using the Augmented Dickey-Fuller (ADF) test. The results indicated that all series were non-stationary, suggesting the presence of unit roots. To address this, the log prices were differentiated once, after which they exhibited stationarity (test are available in Table 4).

These differentiated log returns were then used to calculate the R/S and modified R/S statistics and estimate the Hurst exponent. The purpose of using this data is to evaluate the long-term memory properties of financial markets, which can indicate persistence or mean-reversion in market behavior.

2.5 Results

The following table summarizes the results of the R/S statistic, modified R/S statistic, and the estimated Hurst exponents for each of the five indices analyzed:

Ticker	R/S	Hurst Exponent	Modified Hurst Exponent	Critical Value	Long Memory
S&P 500	30.166	0.558	0.501	1.007	False
Russell 2000	51.373	0.645	0.588	1.714	True
FTSE 100	40.236	0.605	0.548	1.341	False
Nikkei 225	22.234	0.508	0.508	1.048	False
DAX	26.985	0.540	0.540	1.278	False

Table 1 – Results for R/S, Hurst exponent, modified Hurst exponent, critical value at 10%, and rejection of the null hypothesis of no long memory from 1987-09-10 to 2025-02-28. The Hurst exponent can be equal for the R/S and modified R/S methods in the case where the autocorrelation coefficients are less than zero (refer to Section 6.1), in this case we set q equal to 0 and therefore the R/S and modified R/S share the same formula.

Based on the results obtained from applying the traditional R/S method, all the series appear to exhibit long-term memory, as the Hurst exponents are consistently greater than 0.5. However, the unknown asymptotic distribution of the traditional R/S statistic prevents us from determining whether these Hurst values are statistically significant. To address this, we use the modified R/S method, comparing the statistic V to the critical values provided by Lo (1991) (1.620 at the 10% level and 1.747 at the 5% level in a one-tailed test). Our analysis shows that only one series the returns of the Russell 2000 small and mid cap (US) exhibits statistically significant persistence, for the other series, despite Hurst exponents greater than 0.5, the null hypothesis of short memory cannot be rejected.

Since it seems unrealistic to characterize series with only one static Hurst exponent as the series might be influenced by local trends, periods estimations, frequencies and to gain deeper insight into the local scaling dynamics of these series, we now turn to Multifractal Detrended Fluctuation Analysis (MF-DFA). Specifically, MF-DFA allows us to investigate the variety of local behaviors present in the time series by characterizing its multifractal spectrum. This spectrum reveals how "rough" or "smooth" different segments of the series are and indicates the prevalence of each level of irregularity. By examining the multifractal spectrum, we can determine whether the data exhibits a wide range of scaling behaviors, indicative of multifractality, or if it behaves more uniformly. This transition to MF-DFA thus provides a complementary perspective that deepens our understanding of the complex, scale-dependent dynamics governing the indices and how it relates to the dynamisms of the Hurst exponent.

3 Multifractal Detrended Fluctuation Analysis

The Multifractal Detrended Fluctuation Analysis (MF-DFA) is a generalization of the standard Detrended Fluctuation Analysis approach designed to detect multifractality in time series (Kantelhardt et al., 2002). The procedure can be summarized in five steps, as described below:

1. **Profile construction.** Given a series $\{x_k\}_{k=1}^{N}$, we first compute its mean $\bar{x}$. Then, we build the profile
$$Z(i) \;=\; \sum_{k=1}^{i}\big(x_k \;-\; \bar{x}\big), \quad i \;=\; 1, 2, \ldots, N, \tag{13}$$
where we use $Z(i)$ instead of $Y(i)$ to avoid confusion with previous definitions. This cumulative sum helps capture the local fluctuations in the data.

2. **Division into segments.** We split the profile $Z(i)$ into $N_s \equiv \lfloor N/s \rfloor$ non-overlapping segments, each of length s. Since N may not be a multiple of s, we repeat this procedure starting from the opposite end, yielding a total of $2N_s$ segments.

3. **Detrending.** For each of the $2N_s$ segments, we fit a polynomial trend (often linear or quadratic) and subtract it from $Z(i)$ in that segment. Let $z_\nu(i)$ be the fitting polynomial in segment ν. We then define the local variance as
$$F^2\big(s, \nu\big) \;=\; \frac{1}{s}\sum_{i=1}^{s}\Big[Z\big((\nu-1)s + i\big) \;-\; z_\nu(i)\Big]^2. \tag{14}$$
This detrending step removes possible polynomial trends in the data.

4. **Generalized fluctuation function.** For each scale s, we compute the qth-order fluctuation function,
$$F_q(s) \;=\; \left\{\frac{1}{2N_s}\sum_{\nu=1}^{2N_s}\Big[F^2\big(s,\nu\big)\Big]^{q/2}\right\}^{1/q}. \tag{15}$$
Varying q allows us to emphasize large ($q > 0$) or small ($q < 0$) fluctuations.
In the special case $q = 0$, the fluctuation function is defined by a logarithmic averaging (see proof in Appendix Section 6.5):
$$F_0(s) = \exp\left(\frac{1}{4N_s}\sum_{\nu=1}^{2N_s}\ln\Big[F^2\big(s,\nu\big)\Big]\right). \tag{16}$$

5. **Scaling behavior.** Finally, on double-logarithmic axes, we examine the dependence of $F_q(s)$ on s. If

$$F_q(s) \sim s^{h(q)}, \tag{17}$$

then $h(q)$ is called the generalized Hurst exponent. In a multifractal series, $h(q)$ varies with q, indicating different scaling behaviors for large versus small fluctuations.

For monofractal series, $h(q)$ is approximately constant for all q. In contrast, for multifractal series, $h(q)$ strongly depends on q, revealing heterogeneity in the scaling of fluctuations. For a graphical representation of the steps used in the MF-DFA, refer to Figure 10.

3.1 Generalized Hurst Exponent

The S&P 500 and Russell 2000 are ideal candidates for multifractal analysis. The modified R/S statistic (M-R/S) for the S&P 500 is approximately 0.501 very close to 0.5 which suggests that its dynamics are consistent with efficient market behavior. In contrast, the Russell 2000 has a modified Hurst exponent of approximately 0.588, indicating significant long-range dependencies and a less efficient market. Moreover, it is interesting to observe that, in the graphical analysis (refer to Figure 9), there are periods when the S&P 500 displays bullish trends while the Russell 2000 remains relatively flat for no apparent reason.

These discrepancies between the two series highlight their distinct scaling properties and market efficiencies. Our aim with the multifractal analysis is to capture and quantify these differences in local scaling behavior. By analyzing the multifractal spectrum of each index, we hope to match these structural discrepancies, thereby providing deeper insights into the dynamics of each market. By analyzing both the S&P 500 and Russell 2000, we gain insight into how differences in efficiency and persistence affect their multifractal characteristics, thereby allowing us to exploit these structural differences in our trading strategy. For this analysis, we will use the daily returns of the Russell 2000 index, S&P 500 index from September 10th, 1987, to February 28th, 2025 (about 10 000 data points).

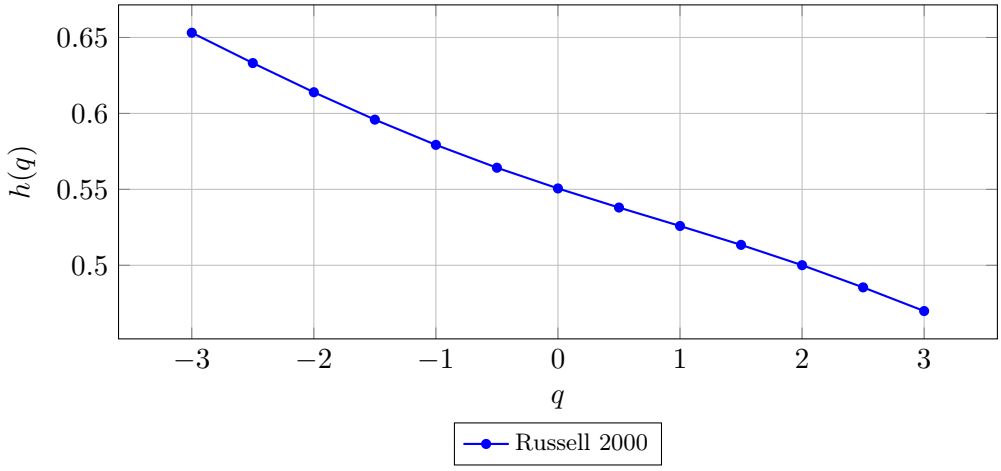

Figure 2 – Generalized Hurst exponent $h(q)$ for the Russell 2000 returns. Values of q are equally spaced between -3 and 3. The scale used are logly spaced between 10 and 500.

If we take a closer look at the results from MF-DFA, we observe that the generalized Hurst exponent, $h(q)$, varies as a function of q. The decrease sloping is a sign that the serie might exhibit multifractal behavior. In a monofractal process, h(q) remains constant, reflecting uniform

scaling. Variation of h(q) with q indicates that small and large fluctuations scale differently. The curvature of the line indicates the presence of heterogeneity in the distribution of singularities, with different regions of the series characterized by varying degrees of irregularity. Lower values of q emphasize small fluctuations, while higher values highlight high fluctuations. Therefore, this spectrum showcases that during periods of small fluctuations (q $<$ 0) the series is likely to exhibit long-term memory as the Hurst exponent is greater than 0.5, whether for drastic changes (q $>$ 0) in the series behavior the Hurst exponent is likely not to be high. This result is consistent with our simulation of the fractional Brownian motion, where we can see that the series exhibits smooth and regular behavior (calm fluctuations) for high Hurst exponent and sharply irregular behavior (high fluctuations) for low Hurst exponent.

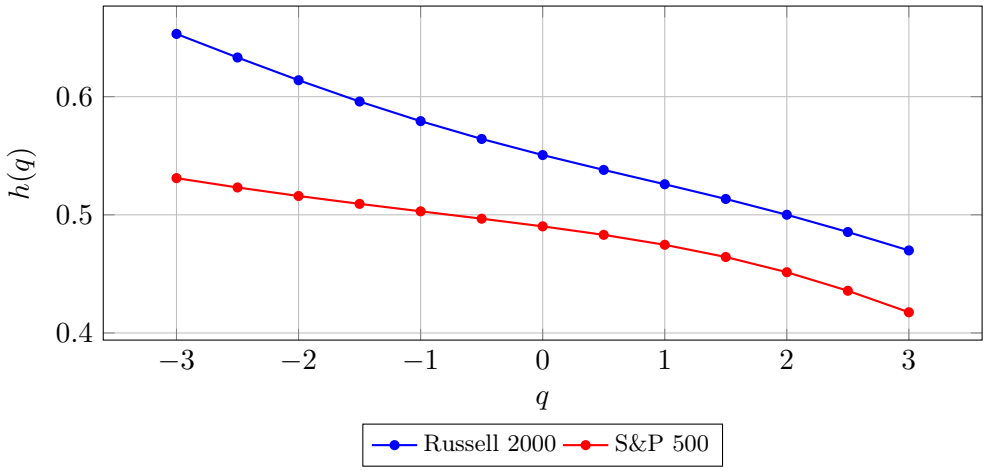

Figure 3 – Generalized Hurst exponent $h(q)$ for the S&P 500 returns. Values of q are equally spaced between -3 and 3. The scale used are logly spaced between 10 and 500.

The multifractal spectrum for the S&P 500 returns exhibits a similar behavior to that of the Russell 2000 returns, except that it is less pronounced. At q = -3, the series exhibits a Hurst exponent of 0.56 compared to 0.65 for the Russell 2000, those series seems to slightly differs in their behavior. This difference, albeit modest, may hint at distinct market microstructure characteristics between the two indices. For instance, the S&P 500, with its larger and more liquid companies, might experience a smoothing effect on return dynamics that could reduce the observable multifractality. In contrast, the Russell 2000, representing smaller-cap stocks, may be subject to greater fluctuations and market inefficiencies, which could amplify multifractal behavior. However, these interpretations remain speculative given the sensitivity of the multifractal analysis to the chosen parameters and evaluation period. Overall, our findings provide an interesting perspective on market behavior, suggesting that although both indices share similar multifractal characteristics, subtle variations exist that could reflect underlying market differences.

From the MF-DFA analysis, we can also compute the Hölder exponent and multifractal spectrum. Calculating the Hölder exponent and multifractal spectrum extends MF-DFA by detailing local behavior. This logical continuation deepens insights into the complex, heterogeneous dynamics of the market.

3.2 Hölder exponent

The Hölder exponent $\alpha(q)$ characterizes the local multifractal strength of a signal and is obtained using the Legendre transform of $h(q)$:

$$\alpha(q) = h(q) + qh'(q). \tag{18}$$

where $h'(q)$ is the derivative of $h(q)$ with respect to q. This exponent quantifies the intensity of local singularities: lower values of α indicate highly irregular (or sharply singular) behavior, while higher values correspond to smoother regions of the signal. Thus, the Hölder exponent reveals the heterogeneity of fluctuations within the signal. This exponent describes the degree of multifractal in different parts of the series, revealing the heterogeneity of fluctuations.

3.3 Multifractal Spectrum

The multifractal spectrum $f(\alpha)$ provides a measure of the fractal dimension of subsets characterized by a given α:

$$f(\alpha) = q[\alpha(q) - h(q)] + 1. \tag{19}$$

This spectrum describes the distribution of singularities in the time series. A wider spectrum indicates stronger multifractality.

The analysis using the Hölder exponent and multifractal spectrum is a powerful tool for studying complex systems. In particular, it enables one to identify and quantify regions of strong multifractal, which may correspond to extreme events or sudden changes in dynamics and to describe the distribution and frequency of irregular behaviors in time series. Thus, the multifractal approach offers a detailed and nuanced description of a signal's local variability, providing essential insights for understanding and predicting its underlying dynamics.

We can distinguish two main contributions to the multifractal spectrum:

$$\mathcal{M}(q) \propto \underbrace{f_{\text{tail}}(q)}_{\substack{\text{Strongly non-Gaussian} \\ \text{distribution}}} \quad \textit{and} \quad \underbrace{f_{\text{corr}}(q)}_{\substack{\text{Temporal correlations} \\ \text{in the series}}}$$

Therefore, in the literature, the multifractality is often reffered as two types :

Type I multifractality arises from a broad probability density function of the series values Jan W. Kantelhardt (2002) and al whereas Type II multifractality stems from long-range correlations within the time series. This distinction enables us to identify and quantify the type of multifractality present. By shuffling the series, we effectively eliminate the long-range correlations, retaining only the influence of the value distribution. In an ideal monofractal series, the Hölder exponent would peak at 0.5 thus, the difference between the exponents of the original and shuffled series reflects the contribution of long-range correlations to the multifractality.

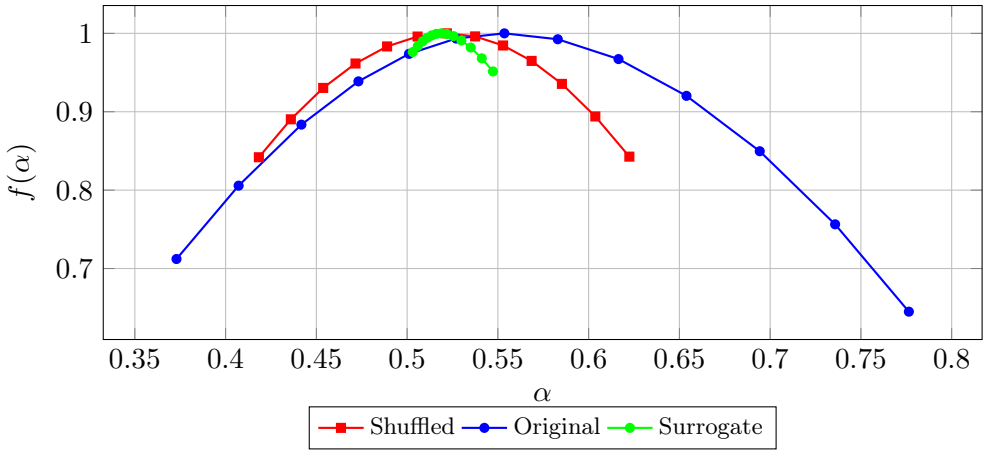

Figure 4 – Multifractal spectrum $f(\alpha)$ for the Russell 2000 returns.

The multifractal spectrum $f(\alpha)$ for the Russell 2000 returns exhibits a bell-shaped curve, indicating multiple scaling behaviors in the data. The peak near the center represents the most common local Hölder exponent, while the spread around this peak highlights the diversity of singularities present in the series. A wider spectrum suggests stronger multifractality, reflecting volatility clustering across multiple timescales and signaling diversified behavior. Furthermore, the approximate symmetry of the curve around its maximum implies that both large and small fluctuations are represented, albeit with varying intensity. Overall, this bell-shaped spectrum underscores the complex, multi-scale nature of the Russell 2000 returns. A peak of the multifractal spectrum at $\alpha \approx 0.55$ indicates that the most common local Hölder exponent in the Russell 2000 returns is around 0.55. In general, $\alpha > 0.5$ suggests a certain degree of smoothness or , $\alpha = 0.5$ aligns with a standard Brownian motion (random walk) where nor smoothness nor irregularity overweigh, and $\alpha < 0.5$ signifies more erratic behavior. Thus, an exponent of 0.55 may implies a moderately rough signal neither purely random nor overly smooth highlighting the presence of multifractal characteristics. Comparing it with the shuffled series, we observe that the α peak is lower than the original series, indicating that the shuffled series exhibits a more uniform behavior with less multifractality. The surrogate version of the series is really narrow meaning that most of the multifractality that we observe are due to the non-gaussian distribution of returns. The multifractality linked to the non-gaussian distribution cannot be quantified as true multifractality since it's due to the finite sample size (Jarosław Kwapień (2023)). The relationship of multifractality are non-linear, therefore the only way to quantifie for each of those sources is via the shuffled and the surrogate one.

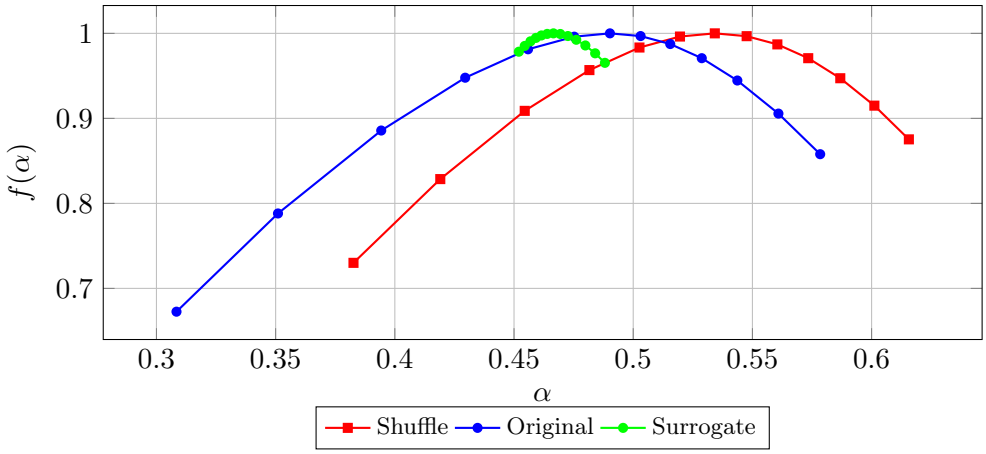

Figure 5 – Multifractal spectrum $f(\alpha)$ for S&P 500 returns.

The multifractal spectrum $f(\alpha)$ for the S&P 500 returns exhibits a different curve shortened on the right side. The spectrum is narrower (0.27 between the maximum and minimum) compared to the Russell 2000 (0.4), suggesting a possibly weaker multifractal nature, the difference between α min and α max is lower than the Russell 2000 ones therefore it implies that the S&P 500 returns exhibit a more uniform behavior compared to the Russell 2000. Let's recall that for a random walk the alpha pic would be close to 0.5 and the spectrum width narrow. The peak near the center for the original series is around 0.486. This may imply that the S&P 500 returns exhibit a more stable behavior compared to the Russell 2000, with less pronounced volatility clustering across multiple timescales. The fact that the curve is shortened on the right but stretches deeper on the left means that the market exhibits fewer ultra-calm intervals in favor of a greater propensity for abrupt or extreme fluctuations otherwise saying that this series exhibit fatter tails. Let's recall that from our analysis with M-R/S, the S&P 500 had a Hurst exponent of 0.501, indicating that the series is likely to be a random walk. Moreover, the α peak of the original series is close to 0.5 (0.486) reinforcing our first result via Hurst. For both series, the width of the spectrum is approximately 0.27, if you look back at the Russell 2000, the width of the spectrum shrinks to 0.2 when shuffling the series, indicating that the multifractality is driven by long-range correlations. In this spectrum, there is no long term correlation, the multifractality is only due to the non-gaussian nature of returns. In the original returns, large jumps cluster together, creating many consecutive "rough" segments with low Hölder exponents. Shuffling breaks up these clusters, so extreme returns become isolated among calmer data. As a result, the modal Hölder exponent shifts upward even though the overall width remains unchanged. Shuffling the series repeatedly won't narrow the spectrum's width; instead, it produces different modal α values. The width of the surrogate is narrower than that of the Russell meaning that for the S&P, the multifractality due to long term correlation is lower.

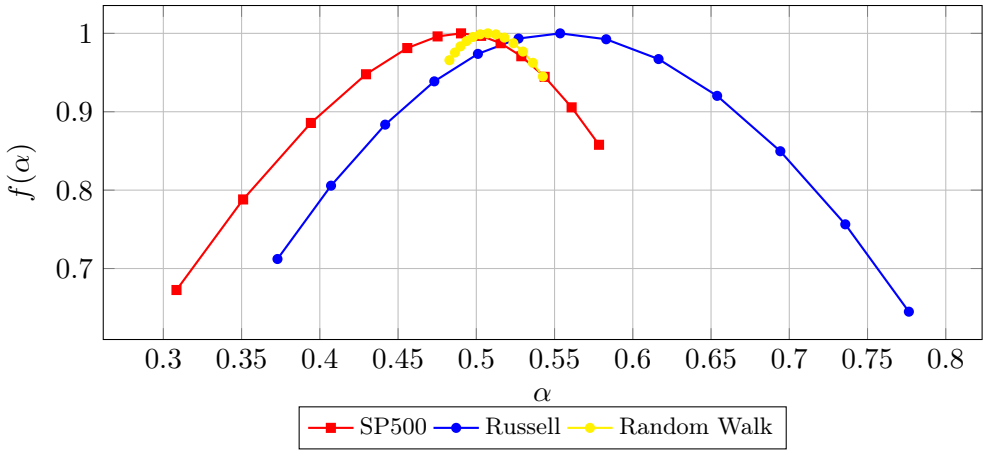

Figure 6 – Comparision of multifractal spectrum for SP500, Russell 2000 and a random walk.

From this analysis, we can conclude that the S&P 500 returns exhibit a behavior close to the one of a random walk and that it's multifractality comes from the non-gaussian nature of the returns (Kurtosis is estimated 28.41) since the width of the spectrum doesn't change much with the shuffling series. Whereas for the Russell 2000 it clearly comes from the long-range correlations (Kurtosis is estimated 12.71) since the width of the spectrum shrinks when shuffling the series. Relationships in multifractality are non-linear and canno't be obtain by calculating a width between two transformed series. The only way to isolate long term correlation is to look at the surrogate series, which is the true sources of multifractality and hence inefficiency.

In an ideal random walk (i.i.d. Gaussian increments), the process is monofractal and the multifractal spectrum collapses to a single point its. It's width $\Delta\alpha$ is close to 0 because every local segment is statistically identical and fully unpredictable. This width therefore quantifies market inefficiency, the larger $\Delta\alpha surrogate$ is, the more the series departs from pure randomness and the more distinct local regimes it contains.

3.4 Proposition of an Inefficiency Index

To capture market inefficiency, we propose combining two key structural components:

1. **Fractal Difference:**

   The width of the multifractal spectrum is defined as

   $$\Delta\alpha = \alpha_{\text{max surrogate}} - \alpha_{\text{min surrogate}}, \tag{20}$$

   where α is the singularity exponent obtained via an MF-DFA analysis.

2. **Deviation of the Rolling Hurst:**

   In an efficient market (i.e., following a Brownian motion) the Hurst exponent is expected to be

   $$H = 0.5. \tag{21}$$

   Therefore, the deviation is measured by

   $$\left|H_{\text{rolling}} - 0.5\right|. \tag{22}$$

We define the inefficiency index I as

$$I = \Delta\alpha_{\text{surrogate}} \times |H_{\text{rolling}} - 0.5|\,, \tag{23}$$

where $\Delta\alpha_{\text{surrogate}}$ is the width between the multifractal spectrum of the surrogate series. It gives us insights on which market seems to be more inefficient due to true long term correlation multifractality.

An efficient market should exhibit

$$H = 0.5, \tag{24}$$

so any deviation quantified by $|H_{\text{rolling}} - 0.5|$ indicates the presence of temporal correlations:

— $H > 0.5$ signals persistence (trends are likely to continue),

— $H < 0.5$ signals anti-persistence (a tendency for mean reversion).

In this framework the moment of order 2 is handled separately via the classical Hurst exponent H, while all higher-order moments are captured through the MF-DFA multifractal spectrum. Using both pieces together gives a more complete and internally consistent picture of market inefficiency: H anchors the second-order dynamics, while MF-DFA reveals any higher-order, non-linear structure that is captured through the surogate series.

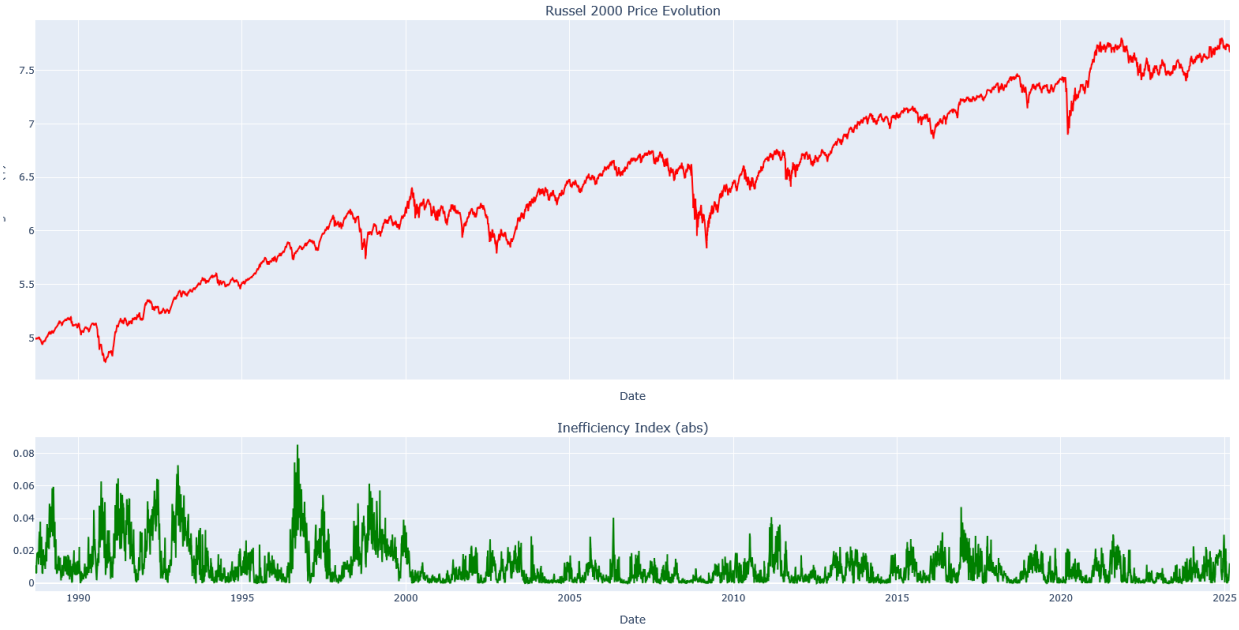

Figure 7 – Log–price trajectory of the Russell 2000.Bottom corresponding inefficiency index $I = \Delta\alpha_{\text{surrogate}} * |H - 0.5|$.

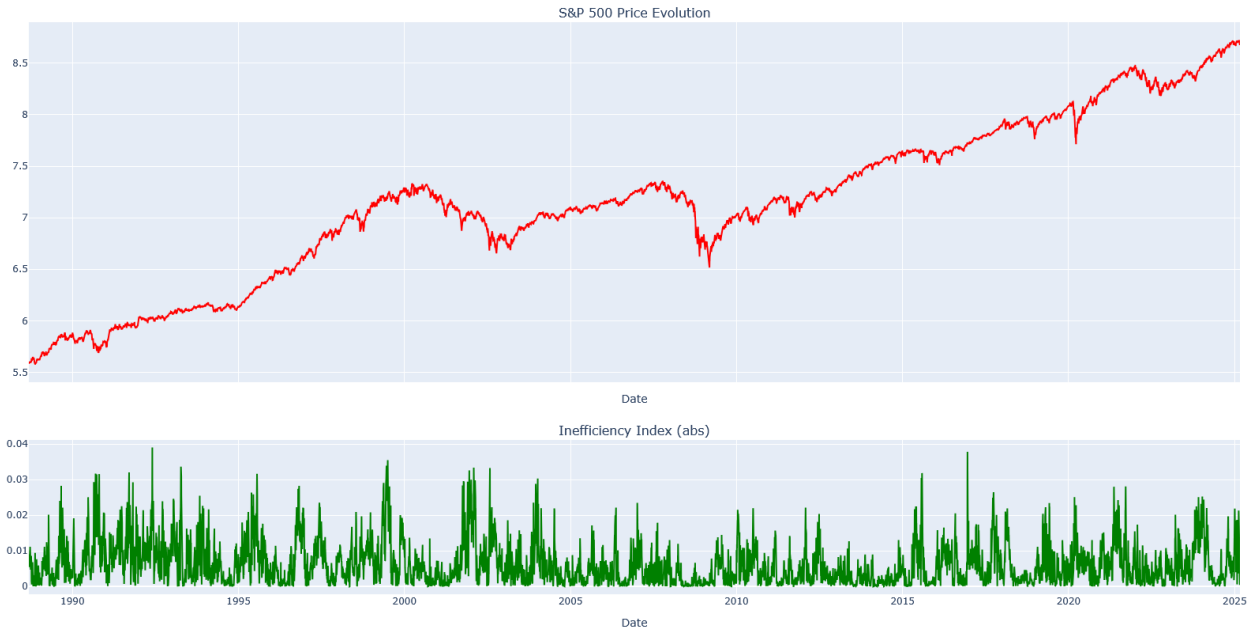

Figure 8 – Log–price trajectory of the S&P 500. Bottom corresponding inefficiency index $I = \Delta\alpha_{\text{surrogate}} * |H - 0.5|$.

	GSPC	RUT	FTSE	N225
GSPC	–	0.13694625448275413	0.00020907545843647192	0.13622507308844675
RUT	0.013187796035365646	–	0.05717962733067387	0.0001200075862534439
FTSE	1.033759053343914e-08	0.06119571156397031	–	0.46972115921790925
N225	0.04566901228083554	0.0010028148307699711	0.6485520380259201	–
GDAXI	0.03382234723520813	0.0018153425678639895	0.12211188804681875	0.055499443168016915

Table 2 – Matrice de corrélation — valeurs arrondies à trois décimales

4 Conclusion

In this paper, we examined the long-term memory and multifractal properties of major stock market indices using both traditional and modified R/S analysis alongside Multifractal Detrended Fluctuation Analysis (MF-DFA). Our findings suggest that, while most series display Hurst exponents greater than 0.5 implying some degree of persistence the modified R/S approach indicates that only the Russell 2000 exhibits statistically significant long memory. In contrast, the S&P 500 shows a more subdued multifractal behavior, with a narrower spectrum and lower extremal Hölder exponents. This difference may reflect underlying market microstructure characteristics, such as liquidity and the size of constituent companies, but these interpretations should be treated with caution. The Hurst exponent seems to be able to capture differences in the multifractal spectrum between the two indices, with the Russell 2000 that appears to display a broader spectrum and more distinct multifractal characteristics compared to the S&P 500. Overall, the outperformance of the strategies seems to hold depending on the window size used, and the proposed inefficiency brings value as a risk limiting filter.

5 Discussion

It is important to emphasize that the methods used in our study both the static Hurst exponent and the multifractal analysis are highly sensitive to the chosen data frequency, evaluation period, and potential structural breaks. The apparent persistence observed in the Russell 2000, for instance, may be influenced by these factors, while the more stable behavior seen in the S&P 500 could result from its larger, more liquid market composition.

Overall, while our results provide an intriguing perspective on market dynamics and offer a foundation for a trading strategy based on these multifractal measures, they should be interpreted with a degree of caution. Future research should aim to extend this analysis to a broader set of assets (pair clustering) and refine the estimation techniques to confirm the statistical significance of the observed multifractal effects.

6 Appendix

Figure 9 – Log cumulative returns of S&P 500 (blue) and Russell 2000 (red) from 1987-09-11 to 2025-02-28. To come back where you left off, see Section 3.1.

6.1 Definition (Time Domain)

A stationary process X_t is said to exhibit long-range dependence (long memory) if there exist constants

$$a \in (0,1), \quad c > 0,$$

such that its autocorrelation function $\rho(k)$ satisfies

$$\lim_{k\to\infty} \frac{\rho(k)}{c\,k^{-\alpha}} = 1 \tag{25}$$

where $\rho(k)$ is the autocovariance function, c is a constant (V.Mignon 2003). To comeback where you left off, see Section 2.5.

6.2 Critical Values for the Modified R/S Test

The critical values for the modified R/S test are provided in the table below. These values are used to assess whether the series exhibits long memory behavior based on the modified R/S statistic.

Significance Level	**critical value (modified R/S Statistic)**
0.005	2.098
0.05	1.747
0.10	1.620

Table 3 – Critical values for the modified R/S Statistic (Lo, 1991). To come back where you left off, see Section 2.3

6.3 Augmented Dickey-Fuller Test

Ticker	P-Value on log prices	P-Value on log differentiated return
S&P 500	0.863	0.000
Russell 2000	0.695	0.000
FTSE 100	0.226	0.000
Nikkei 225	0.660	0.000
DAX	0.663	0.000

Table 4 – P-values from the Augmented Dickey-Fuller (ADF) test for stationarity. The P-value of log prices refers to the Augmented Dickey Fuller test (ADF) on log prices, while the P-value of log-differentiated prices indicates the ADF test on log-differentiated returns. The null hypothesis is non-stationarity. To come back where you left off, see Section 2.4

6.4 Demonstration of the covariance of fractional Brownian motion (fBm)

The fractional Brownian motion (fBm), denoted by $X_H(t)$, is defined as a zero-mean continuous-time Gaussian process whose increments are correlated. Its covariance function is given by:

$$C_H(t,s) = \frac{\sigma^2}{2}\left(t^{2H} + s^{2H} - |t-s|^{2H}\right)$$

where $H \in (0,1)$ is the Hurst exponent.

A fractional Brownian motion $X_H(t)$ with $X_H(0) = 0$ has increments that are normally distributed with zero mean, specifically:

$$X_H(t) - X_H(s) \sim \mathcal{N}(0, \sigma^2|t-s|^{2H})$$

Given that the process is centered (zero mean), the covariance is defined as:

$$C_H(t,s) = \text{Cov}(X_H(t), X_H(s)) = \mathbb{E}[X_H(t)X_H(s)]$$

Using the following algebraic identity:

$$X_H(t)X_H(s) = \frac{1}{2}\left[X_H(t)^2 + X_H(s)^2 - (X_H(t) - X_H(s))^2\right]$$

the covariance becomes:

$$C_H(t,s) = \frac{1}{2}\left(\mathbb{E}[X_H(t)^2] + \mathbb{E}[X_H(s)^2] - \mathbb{E}[(X_H(t) - X_H(s))^2]\right)$$

We have by definition of fBm:

$$\mathbb{E}[X_H(t)^2] = \sigma^2 t^{2H}, \quad \mathbb{E}[X_H(s)^2] = \sigma^2 s^{2H}, \quad \mathbb{E}[(X_H(t) - X_H(s))^2] = \sigma^2 |t-s|^{2H}$$

Substituting these into our covariance expression, we get:

$$C_H(t,s) = \frac{1}{2}\left(\sigma^2 t^{2H} + \sigma^2 s^{2H} - \sigma^2 |t-s|^{2H}\right)$$

Factoring out the term σ^2, we arrive at the final covariance formula:

$$\boxed{C_H(t,s) = \frac{\sigma^2}{2}\left(t^{2H} + s^{2H} - |t-s|^{2H}\right)}$$

This covariance function entirely characterizes the dependence structure of fractional Brownian motion, revealing long-term correlation when $H > 0.5$ (persistence) and anti-correlation when $H < 0.5$ (anti-persistence). To comeback where you left off, see Section 3.

6.5 MF-DFA Analysis

Proof of $F_0(s)$ as $q \to 0$

$$F_q(s) = \left[\tfrac{1}{2N_s}\sum_{v=1}^{2N_s}\left(F_v^2(s)\right)^{q/2}\right]^{1/q} \implies \ln F_q(s) = \frac{1}{q}\ln S(q),$$

where

$$S(q) = \frac{1}{2N_s}\sum_{v=1}^{2N_s} e^{\frac{q}{2}\ln F_v^2(s)}.$$

As $q \to 0$, $\ln S(q) \to 0$ and we apply L'Hôpital:

$$\lim_{q\to 0}\ln F_q(s) = \lim_{q\to 0}\frac{\ln S(q)}{q} = \left.\frac{S'(q)}{S(q)}\right|_{q=0} = \frac{1}{4N_s}\sum_{v=1}^{2N_s}\ln F_v^2(s).$$

Exponentiating:

$$F_0(s) = \exp\Big[\tfrac{1}{4N_s}\sum_{v=1}^{2N_s}\ln F_v^2(s)\Big] = \exp\Big[\tfrac{1}{2N_s}\sum_{v=1}^{2N_s}\ln F_v(s)\Big].$$

Thus $F_0(s)$ is the geometric mean of the segment fluctuations. To comeback where you left off, see Section 3.

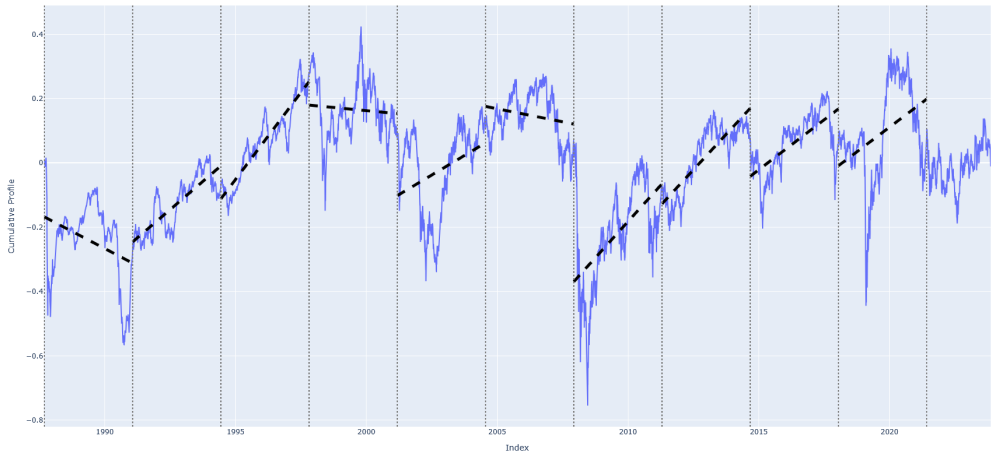

Figure 10 – Simulation of the MF-DFA steps, the series is the Russell 2000 returns split into segments of length 880. The blue line represents the cumulative sum of the centered returns, while the coloured lines represent the polynomial fit for each segment. To come back where you left off, see Section 3.

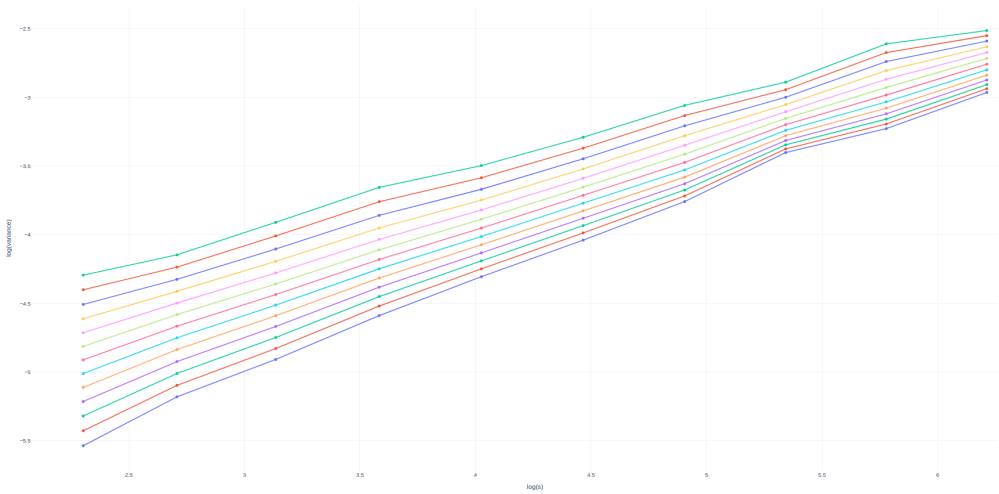

Figure 11 – Plot of the log scales (10 logly spaced increments from 10 to 500) against the log variance for each values of q, green line (highest line) represents q = -3 the lowest line represents q = 3. The slope of the line is the Hurst exponent for each q.

6.6 Ex-post analysis of the portfolio performance

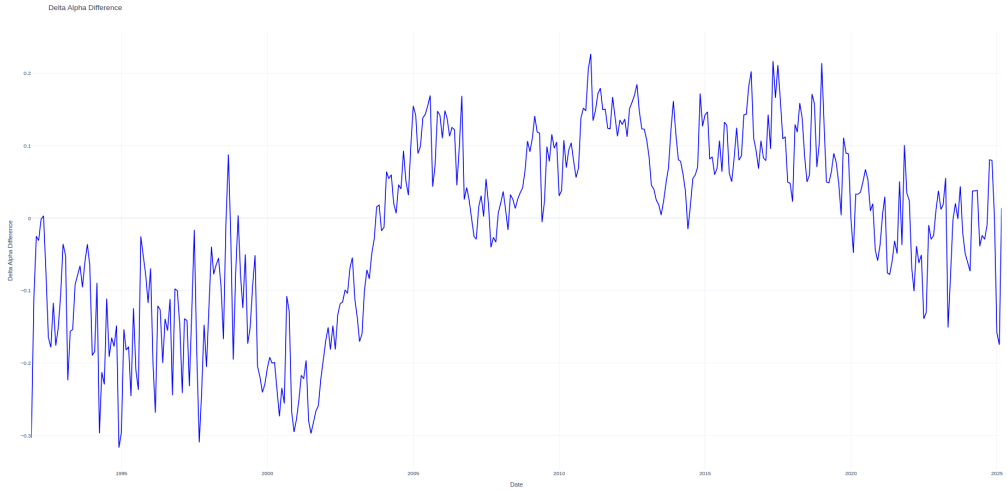

Figure 12 – Rolling alpha width difference computed with a rolling window of 1008 days (4 years) for the S&P 500 and Russell 2000. The data in this example is resampled to monthly for better clarity.

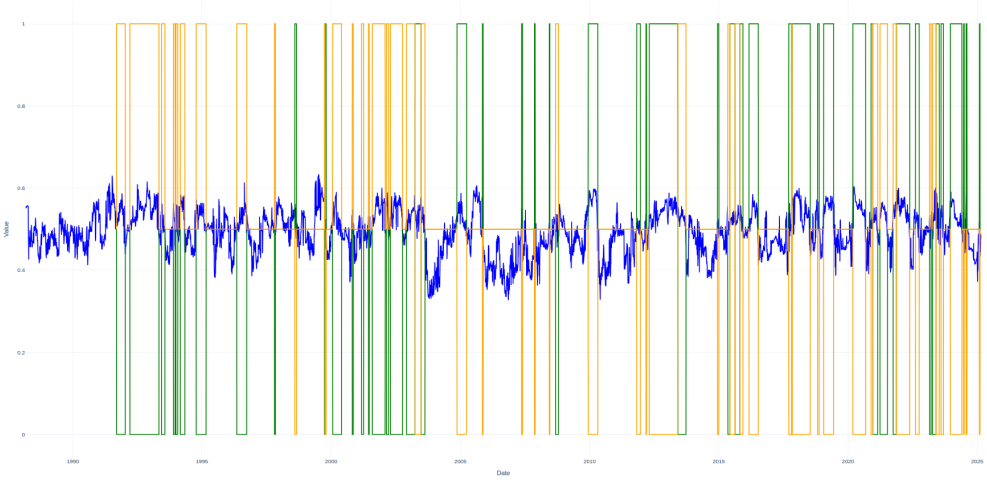

Figure 13 – Composition of our portfolio (Russell 2000 in yellow, S&P 500 in green) based on the inefficiency index, the blue line corresponds to the modified rolling hurst with a rolling window of 120 days. The position start to change in 1991-10-18 because we need 4 years of data to compute the $\Delta\alpha_{\text{diff}}$. The portfolio is long only and the weights are adjusted daily. To comeback where you left off, see Section **??**.

6.7 Backtest different rolling window size results

Strategy	Annualized Return	Annualized Volatility	Sharpe	Max Drawdown
TradOverlap120	9.797	19.402	0.505	-56.987
Long Only SP500	8.196	17.875	0.458	-56.775
Long Only Russell	7.368	21.726	0.339	-59.889
50/50 Portfolio	7.941	19.134	0.415	-57.993

Table 5 – 1991-11-15 to 2025-02-28 | Window size 120 days. Traditional R/S method is used here To comeback where you left off, see Section **??**.

Strategy	Annualized Return	Annualized Volatility	Sharpe	Max Drawdown
ModifOverlap252	9.218	19.388	0.475	-57.87
Long Only SP500	8.196	17.875	0.458	-56.775
Long Only Russell	7.368	21.726	0.339	-59.889
50/50 Portfolio	7.941	19.134	0.415	-57.993

Table 6 – 1991-11-15 to 2025-02-28 | Window size 252 days

Strategy	Annualized Return	Annualized Volatility	Sharpe	Max Drawdown
ModifOverlap504	8.657	19.452	0.445	-57.138
Long Only SP500	8.196	17.875	0.458	-56.775
Long Only Russell	7.368	21.726	0.339	-59.889
50/50 Portfolio	7.941	19.134	0.415	-57.993

Table 7 – 1991-11-15 to 2025-02-28 | Window size 504 days

Strategy	Annualized Return	Annualized Volatility	Sharpe	Max Drawdown
ModifOverlap1260	9.022	19.48	0.463	-56.461
Long Only SP500	8.228	17.995	0.457	-56.775
Long Only Russell	7.471	21.905	0.341	-59.889
50/50 Portfolio	8.01	19.284	0.415	-57.993

Table 8 – 1992-08-22-2025-02-28 | Window size 1260 days

Strategy	Annualized Return	Annualized Volatility	Sharpe	Max Drawdown
ModifOverlap2520	7.278	20.824	0.349	-55.982
Long Only SP500	6.852	19.043	0.36	-56.775
Long Only Russell	6.148	23.417	0.263	-59.889
50/50 Portfolio	6.673	20.563	0.325	-57.993

Table 9 – 1997-06-18-2025-02-28 | Window size 2520 days

7 References

Lo, A.W. (1991). *Long-Term Memory in Stock Market Prices*.

Mignon, V. (2003). *Méthodes d'estimation de l'exposant de Hurst. Application aux rentabilités boursières*, Économie & Prévision.

Kantelhardt, J.W., Zschiegner, S.A., Koscielny-Bunde, E., Bunde, A., Havlin, S., & Stanley, H.E. (2002). *Multifractal Detrended Fluctuation Analysis of Nonstationary Time Series. Physica A: Statistical Mechanics and its Applications*, 316(1–4), 87–114.

Lukasz Czarnecki, Dariusz Grech, Multifractal dynamics of stock markets, 2009, Acta Physica Polonica Series.

Genuine multifractality in time series is due to temporal correlations, 2023 (Jarosław Kwapień)

Andrews, D.W.K. (1991). *Heteroskedasticity and Autocorrelation Consistent Covariance Matrix Estimation*. *Econometrica*, 59(3), 817-858.

Mandelbrot, B.B. and Wallis, J.R. (1968). "Noah, Joseph, and Operational Hydrology", *Water Resources Research*, vol. 4, pp. 909–918.

Mandelbrot, B.B. (1973). "Le problème de la réalité des cycles lents et le syndrome de Joseph", *Economie Appliquée*, vol. 26, pp. 349–365.

Mandelbrot, B.B. and Wallis, J.R. (1969a). "Some Long-Run Properties of Geophysical Records", *Water Resources Research*, vol. 5, pp. 321–340.

Mandelbrot, B.B. and Wallis, J.R. (1969b). "Robustness of the Rescaled Range R/S in the Measurement of Noncyclic Long-Run Statistical Dependence", *Water Resources Research*, vol. 5, pp. 967–988.

Mandelbrot, B.B. and Taqqu, M.S. (1979). "Robust R/S Analysis of Long-Run Serial Correlation", *Bulletin of the International Statistical Institute*, vol. 48, pp. 69–104.